Published in final edited form as:
Dev Biol. 2010 April 1; 340(1): 10–21. doi:10.1016/j.ydbio.2010.01.008.

Dicer Inactivation in Osteoprogenitor Cells Compromises Fetal Survival and Bone Formation, While Excision in Differentiated Osteoblasts Increases Bone Mass in the Adult Mouse

Tripti Gaur[a], **Sadiq Hussain**[a], **Rajini Mudhasani**[a], **Isha Parulkar**[a], **Jennifer L. Colby**[a], **Dana Frederick**[a], **Barbara E. Kream**[b], **Andre J. van Wijnen**[a], **Janet L. Stein**[a], **Gary S. Stein**[a], **Stephen N. Jones**[a], and **Jane B. Lian**[a,*]

[a] Department of Cell Biology and Cancer Center, University of Massachusetts Medical School, Worcester, MA, 01655

[b] Department of Medicine, University of Connecticut Health Center, Farmington, CT 06030-1850

Abstract

MicroRNA attenuation of protein translation has emerged as an important regulator of mesenchymal cell differentiation into the osteoblast lineage. A compelling question is the extent to which miR biogenesis is obligatory for bone formation. Here we show conditional deletion of *Dicer* in osteoprogenitors by *Col1a1*-Cre compromised fetal survival after E14.5. A mechanism was associated with the post-commitment stage of osteoblastogenesis, demonstrated by impaired ECM mineralization and expression of mature osteoblast markers in ex vivo deleted Dicer$^{c/c}$ during differentiation of mesenchymal cells. In contrast, in vivo excision of *Dicer* by *Osteocalcin*-Cre in mature osteoblasts generated a viable mouse with a perinatal phenotype of delayed bone mineralization which was resolved by 1 month. However, a second phenotype of significantly increased bone mass developed by 2 months, which continued up to 8 months in long bones and vertebrae, but not calvariae. Cortical bone width and trabecular thickness in Dicer$^{\Delta oc/\Delta oc}$ was twice that of Dicer$^{c/c}$ controls. Normal cell and tissue organization was observed. Expression of osteoblast and osteoclast markers demonstrated increased coupled activity of both cell types. We propose that Dicer generated miRs are essential for two periods of bone formation, to promote osteoblast differentiation before birth, and control bone accrual in the adult.

Keywords

Dicer ablation; microRNAs; bone formation; Col1a-Cre; osteocalcin-cre; high bone mass; osteoblast differentiation; bone development

INTRODUCTION

For normal development of a mineralized skeleton and renewal of bone throughout life, membranous and endochondral bone formation are tightly regulated by osteogenic signaling

*Corresponding Author: Jane B. Lian, Department of Cell Biology, University of Massachusetts Medical School, 55 Lake Avenue North, Worcester, MA 01655, Tel: 508-856-5625; Fax: 508-856-6800; jane.lian@umassmed.edu.

pathways (Wnt, TGFβ/BMP, Notch) and transcription factors directing cell specification (Lian et al., 2006; Soltanoff et al., 2009). Following commitment of mesenchymal stem cells to osteoprogenitors, further differentiation requires the temporal activation of genes coding proteins responsible for forming the bone ECM, promote mineralization and support the metabolic activities of osteoblasts. Gene regulatory mechanisms essential for bone formation have been elaborated in relation to epigenetic and chromatin alteration of the gene, post-transcriptional control of mRNA from splice variants and post-translational biochemical modifications of protein activity. The regulatory function of microRNA (miR), the small non-coding RNA molecules that regulate gene expression through post-transcriptional degradation or translational inhibition by binding to their target mRNAs, in controlling levels and/or translation of target mRNAs during *in vivo* bone formation has not been examined.

Only a small number of miRs that function during skeletal development and in relation to disease have been identified (Kobayashi et al., 2008; Li et al., 2009; Luzi et al., 2008; Mizuno et al., 2008a; Nakasa et al., 2008). MicroRNAs have been characterized in bone and cartilage and in association with rheumatoid arthritis synovial tissue (Kobayashi *et al.*, 2008; Li et al., 2008b; Luzi *et al.*, 2008; Mizuno et al., 2008b; Nakasa *et al.*, 2008; Tuddenham et al., 2006). Significantly, two studies identified miRs which were both modulated at the onset of induced osteoblastogenesis by BMP2 in human mesenchymal stromal cells and C2C12 myogenic cells (Li *et al.*, 2008b; Oskowitz et al., 2008). Profiling of BMP2 during bone formation in vivo (Kobayashi et al., 2008) and during stages of osteoblast differentiation in vitro (Li et al., 2009) has also implicated mature miRs in the regulation of transcripts that contribute to skeletal activities. In addition to these studies in bone forming osteoblasts, miRs regulating the bone resorbing osteoclasts are now known (Sugatani and Hruska, 2009). These findings raise a compelling question as to the requirement for miRs contributing to activation of bone formation and regulating suppression of the osteoblast phenotype in non-osseous cells. Here we addressed whether miRs are required for activation of bone formation and maintenance of osteoblast function in vivo.

One approach for understanding tissue specific requirements for miRs is the conditional deletion of the enzymes Drosha and Dicer (Bernstein et al., 2003). The Drosha process requires the primary miRNAs encoded in genes to 60–70 nucleotide long precursor miRNA (pre-miRNA) in the cytoplasm which are recognized and cleaved by a RNase III endonuclease protein, Dicer, to generate 21–23 nucleotide mature miRNAs that assemble into a ribonucleoprotein silencing complex (RISC) to bind to 3′ untranslated region (UTR) of the target mRNAs (Jaskiewicz and Filipowicz, 2008). Dicer plays a critical role in a vast range of physiologic processes, including embryonic development, cell growth and phenotype differentiation through regulation of microRNA maturation (Blakaj and Lin, 2008). Dicer functions are essential for embryo development and survival as a Dicer-null (Bernstein *et al.*, 2003) and a hypomorphic Dicer mutant (Yang et al., 2005) results in lethality in the first week of embryogenesis. Thus, conditional ablation of Dicer activity has been studied in various tissues, demonstrating a pivotal role of Dicer-dependent processing of microRNAs for cell fate specification, differentiation and tissue morphogenesis in all the tissues examined, among which include skin follicles, heart, brain, immune cells, lung, spermatogenesis and female germline cells (Andl et al., 2006; Chen et al., 2008; Cobb et al., 2005; da Costa Martins et al., 2008; Damiani et al., 2008; Davis et al., 2008; Harris et al., 2006; Harvey et al., 2008; Hayashi et al., 2008; Kanellopoulou et al., 2005; Koralov et al., 2008; Muljo et al., 2005; Murchison et al., 2007; Nagaraja et al., 2008; O'Rourke et al., 2007; Schaefer et al., 2007; Yi et al., 2006).

Limited information is available for Dicer and microRNA requirements during skeletal development. Limb mesoderm-specific deletion of *Dicer* using *prx1*-Cre in mice resulted in massive cell death and reduction in size, but did not affect skeletal patterning (Harfe et al., 2005). However, the requirement for Dicer processed mature miRs in bone tissue has remained

unexplored. In this study, excision of *Dicer* in mice was performed at two stages of bone formation using *Col1a1*-Cre and *Osteocalcin* (*OC*)-Cre which resulted in distinct phenotypes identifying different requirements for miR biogenesis. Ablation of Dicer in osteoprogenitors (using Col1a1-Cre for conditional deletion) prevents their differentiation and compromises fetal survival at E15.5. *OC*-Cre excision of *Dicer* delays perinatal bone formation which is resolved during post-natal growth. However, in $Dicer^{\Delta oc/\Delta oc}$ adult mice a striking increase in both trabecular and cortical bone mass was found. This deregulated increase in bone tissue formation was accompanied by a coupled increase in bone resorption to support vascularization of the thickened bone. A contributing mechanism to this anabolic phenotype is the increased synthesis of bone matrix proteins including collagen type I, a target of several microRNAs in osteoblasts. Our studies establish that miRs are required to initiate osteoblast maturation during development and to regulate bone mass in adult mice.

MATERIALS AND METHODS

Conditional excision of *Dicer*

For conditional deletion of *Dicer*, $Dicer^{c/c}$ mice (Mudhasani et al., 2008) were crossed with *Col1a1*-Cre (2.3 kb promoter of *collagen type I*) (Liu et al., 2004) and *OC*-Cre (*Osteocalcin*) (Chiang et al., 2009; Yuan et al., 2008) mouse line obtained from Dr. Thomas Clemens (University of Alabama at Birmingham, AL). $Dicer^{c/c}$ mice were crossed with *Ink4a/Arf* $^{-/-}$ mice for deletion of the *Ink4a/Arf* locus to obtain senescence-resistance (Serrano et al., 1996). The mice were maintained at the University of Massachusetts by IACUC approved procedures. Genotyping was carried out as previously described (Chiang *et al.*, 2009; Liu *et al.*, 2004; Mudhasani *et al.*, 2008).

MicroCT (μCT) analysis

MicroCT analysis was performed by the University of Massachusetts Medical School Musculoskeletal Center for Imaging Core facility. Bones were fixed in periodate-lysine-paraformaldehyde (PLP) fixative (Miao and Scutt, 2002) from 4 and 8-week-old $Dicer^{c/c}$ and $Dicer^{\Delta oc/\Delta oc}$ mice (n=2 mice per group). After dehydration to 70% alcohol, femurs were scanned at 10 μm voxel resolution (μCT 40; Scanco Medical AG, Bruttisellen, Wangen-Brüttisellen, Switzerland). Image reconstruction was performed by Scanco software version 5.0. For trabecular bone 100 contiguous slices below the growth plate were selected for contouring inside the endosteal edge for analyses of various bone parameters. Cortical parameters were analyzed from 50 cross-sectional slices at the mid-diaphysis region. Parameters were obtained using thresholds range 220–1000.

Skeletal staining and histology

Whole skeletal staining was performed by standard procedures using Alcian blue and Alizarin red stains for cartilage and bone tissue (Lufkin et al., 1992). Separate embryos or day 2 pups were fixed in PLP, paraffin-embedded, and sequential staining of sections was performed by von Kossa stain for mineral and Toluidine blue for cellular detail. Cytochemical detection of bone-specific alkaline phosphatase (Alk Phos) and osteoclast-specific tartrate resistant acid phosphatase (TRAP) was performed (Lengner et al., 2004). Images were captured using a Zeiss Axioskop 40 (Mikron, San Marcos, CA, USA) microscope with a CCD camera.

Ex vivo osteoblast differentiation

Bone marrow stromal cells (BMSC) were isolated from $Dicer^{c/c}$ mice in αMEM supplemented with 20% fetal bovine serum (Hyclone, Logan, UT, USA). Cells were transduced at 60% confluency with Ad-Cre or Ad-GFP (control virus) for 3 h for excision of *Dicer*, then cultured in αMEM with 50 μg/ml ascorbic acid and 10 mM β-glycerol phosphate (SIGMA-Aldrich, St.

Louis, MO, USA) to induce the osteoblast differentiation. Calvarial osteoblasts were isolated from newborn $Dicer^{\Delta oc/\Delta oc}$ by collagenase P digestion, genotyped and cultured for osteoblast differentiation (Pratap et al., 2003). Cells were harvested at indicated time points for Alk Phos activity, mineral staining, and gene expression analyses. Staining for senescence associated β-Galactosidase (SA-βGal) was performed by a standard procedure (Dimri et al., 1995). Excision of *Dicer* was detected by PCR with forward (5′-CCGACCAGCCTTGTTACCTG-3′) and reverse primers (5′-CGGTGTTTCCTTTGAATACTT-3′) using GAPDH as internal control (Applied Biosystems). Experiments were repeated at least twice with similar results.

RNA isolation and quantitative real time PCR

Cells were harvested in 300 μl TRIzol reagent (Invitrogen, Carlsbad, California, USA). Total RNA isolated as per the manufacturer's instructions (Invitrogen, Carlsbad, California, USA) and treated with RNase-free DNase. The reverse transcription reaction was performed on 1 μg of RNA using the First Strand Synthesis Kit (Invitrogen, Carlsbad, California, USA). Relative transcript levels were measured by quantitative PCR in 25 μl reaction volume using ABI PRISM 7300 sequence detection system (Applied Biosystems, Foster City, CA, USA), following the recommended protocol for SYBR-Green, and normalized with GAPDH levels (Applied Biosystems, Foster City, CA, USA). The primers used for amplification are described in Table 1.

For detection of let-7a and miR-29b, mirVANA qRT-PCR miRNA detection kit along with primer sets for each microRNA (Applied Biosystems/Ambion, Foster City, CA, USA) were used, following the manufacturer's procedure. The miR levels were normalized using U6 primers.

RESULTS

In vivo deletion of *Dicer* in hypertrophic chondrocytes and osteoblast lineage cells induces embryonic lethality

To establish the role of Dicer-dependent miRs in bone growth and differentiation, we used a *Dicer* conditional mouse model ($Dicer^{c/c}$) in which Cre-mediated excision leads to deletion of the Dicer PAZ domain (Mudhasani et al., 2008). The *collagen type 1* (2.3 kb) promoter driving Cre recombinase (*Col1a1*-Cre) which is robustly expressed in committed osteoprogenitors, osteoblasts and hypertrophic chondrocytes (Liu et al., 2004) was used to address Dicer functions during skeletal development. Because no live mice with homozygous deletion of *Dicer* were recovered at birth, embryos were examined for skeletal deformities. At E14.5 Cre-positive $Dicer^{\Delta col1/\Delta col1}$ fetal pups represented 24% of the total population of 49 embryos from 8 litters and were smaller but viable (Fig. 1A, upper panels). Skeletal staining, however, revealed a deformed cartilage skeleton without bone tissue in $Dicer^{\Delta col1/\Delta col1}$, whereas $Dicer^{c/c}$ embryos showed early bone formation (Fig. 1A, lower panels). E15.5 $Dicer^{\Delta col1/\Delta col1}$ pups represented 23% of the population but were partly resorbed (Fig. 1B). Thus, after E14.5 fetal survival is compromised by *Dicer* excision.

We analyzed cellular details of $Dicer^{c/c}$ and $Dicer^{\Delta col1/\Delta col1}$ fetal pups to identify specific functions of Dicer during embryonic bone development. In control mice at E14.5 (Fig. 1C) intramembranous and endochondral bone formation was detected by mineral deposition and alkaline phosphatase (Alk Phos) positive osteoblasts and hypertrophic chondrocytes in the mandible, clavicles and ribs (Fig. 1D, 1–4). In $Dicer^{\Delta col1/\Delta col1}$ embryos, bone tissue was either completely absent or significantly reduced as reflected by fewer Alk Phos positive cells. Mineralized tissue formation appears to be compromised as no von Kossa staining occurred in cartilaginous or osseous tissues (Fig. 1D, 5–8). Thus, Dicer ablation by *Col1a1*-Cre inhibits

further differentiation of committed osteoblasts between E14.5 and E15.5, when there is a rapid induction of mineralizing elements in control mice.

Fetal lethality at the onset of bone formation that results from lack of Dicer in *Col1a1* expressing cells may be due in part because a marrow cavity, which supports hematopoiesis, is not formed. Alternatively, bone formation may only be delayed in the absence of Dicer; however, lethality at E15.5 does not allow this assessment. We conclude loss of miR processing at E14.5 prevents maturation to hypertrophic chondrocytes and osteoblasts that results in failure to produce mineralized matrices.

Ex vivo Deletion of *Dicer* abrogates miR processing and results in defective osteoblast differentiation

To identify the stage of osteoblastogenesis blocked in $Dicer^{\Delta col1/\Delta col1}$ mice, bone marrow stromal cells (BMSCs) from $Dicer^{c/c}$ mice at 8 weeks were differentiated into the osteoblast lineage. Following transduction of BMSCs by adenovirus Cre (Ad-Cre), the *Dicer* locus showed >90% excision (Fig. 2A). To confirm loss of miRs, we examined miR-29b and let-7a expression (Fig. 2B), which are known to influence osteoblast differentiation and tissue formation (Harfe *et al.*, 2005;Li *et al.*, 2009). We find that in differentiating control Ad-GFP cells, miR-29b and let-7a are upregulated at the matrix maturation stage (day 19) and downregulated during mineralization (day 27). In Dicer ablated cells, let-7a levels were suppressed throughout differentiation (Fig. 2B), indicating loss of miRs in the absence of Dicer. No difference in cellularity was observed between Ad-GFP and Ad-Cre treated cells from initial plating to confluency, as shown by Toluidine blue staining at day 5 (Fig. 2C) and normal expression of histone H4 RNA (Supplementary Fig. S1A). Also, pro-apoptotic Bax and anti-apoptotic Bcl2 were expressed at comparable levels in both GFP control and Ad-Cre treated samples (Supplementary Fig. S1B) suggesting normal growth and survival properties in absence of Dicer in BMSCs. While control cells exhibited the normal differentiation profile of increased Alk Phos and ECM mineralization (Fig. 2C, upper panels), BMSCs lacking Dicer activity (Ad-Cre) showed markedly reduced Alk Phos activity and mineral deposition as early as day 12, reflecting failed maturation (Fig. 2C, lower panels).

The mechanism of inhibited differentiation was interrogated by examining expression of genes that contribute to osteoblast maturation. *Runx2*, the early marker of a committed osteoblast, and *Col1a1* are equivalently expressed between Ad-GFP and Ad-Cre cultures at day 12 and 19 (for *Col1a1*). However, neither *Runx2* nor *Col1a1* is further upregulated in Ad-Cre cells as differentiation progresses (Fig. 2D). Markers related to mineral deposition, *Alk Phos*, *Osteopontin (OP)*, *Osteocalcin* and *Bone sialoprotein (BSP)* were not induced in Dicer-ablated cells (Fig. 2D). Our results show that osteoblast defects occur after cells are committed to the bone phenotype by Run×2; thus, evidence is provided that commitment and proliferative expansion of osteoprogenitors are not affected by *Dicer* excision in BMSCs. These findings suggest that a group of miRs processed by Dicer are required for maturation to the fully differentiated osteoblast phenotype.

Absence of Dicer induces differentiation defects independent of cell senescence

Recent reports indicate an increase in senescence of mouse embryonic fibroblasts upon Dicer deletion (Mudhasani et al., 2008). To explore the possibility of a similar secondary effect in BMSCs, we performed senescence-associated β-Gal staining on growing cells after *Dicer* excision by Ad-Cre. Increased senescence was observed in *Dicer*-ablated cells compared to control cells by histochemical staining (Fig. 3A, left panel) and confirmed by 2.4 fold higher expression of p21, a marker of senescence (Fig. 3A, right panel). To exclude a role for cell senescence in reduced osteogenesis of *Dicer*-ablated cells, BMSCs were obtained from $Dicer^{c/c}$; $Ink4a/Arf^{-/-}$ mice for osteoblast differentiation following treatment with Ad-GFP

(control) and Ad-Cre. Analyses were performed on day 7 post infection. An 80% reduction of *Dicer* mRNA was found in BMSCs infected with Ad-Cre (Fig. 3B). Also, p21 expression by qRT-PCR confirmed that osteoblast cell senescence is not affected by Dicer excision in BMSCs from senescence resistant mice (Fig. 3B). Dicer-ablated BMSCs could not undergo matrix maturation and mineralization based on inhibited Alk Phos, mineral deposition, and *OC* mRNA levels (Fig. 3B). Thus, removal of senescence did not rescue Dicer-induced differentiation defects. This strengthens the conclusion that defects in osteoblast differentiation are not secondary to premature cell death, but are directly related to absence of miRs.

Deletion of *Dicer* in osteoblasts and osteocytes delays perinatal bone formation

Osteocalcin is highly expressed in mature surface osteoblasts and osteocytes. To further explore in vivo mechanisms for Dicer control of bone formation during mineralization, we inactivated Dicer by *OC*-Cre which is robustly expressed in mature osteoblasts in a matrix undergoing active deposition of mineral (Chiang *et al.*, 2009; Yuan *et al.*, 2008). $Dicer^{\Delta oc/\Delta oc}$ mice were viable, with no apparent skeletal defects at birth by skeletal staining and radiography (data not shown). Femur histology (day 2 mice) showed normal cellular organization of the growth plate and bone formation (data not shown). However, we observed a delay in endochondral bone formation in the tail vertebrae, which are the last bones to develop. $Dicer^{\Delta oc/\Delta oc}$ vertebrae had fewer hypertrophic chondrocytes and weaker Alk Phos activity in the bone collar compared to $Dicer^{c/c}$ (Figs. 4A, 1, 2). Therefore, we examined the fetal skeleton at E17.5 and found that the craniofacial region and ribs displayed strikingly reduced Alk Phos activity in $Dicer^{\Delta oc/\Delta oc}$ (Figs. 4A, 3–6). These results suggest delayed bone formation and an inherent defect in osteoblastogenesis.

Cellular mechanisms for $Dicer^{\Delta oc/\Delta oc}$ induced bone defects were examined by *ex vivo* differentiation of calvarial osteoblasts from newborn mice. A severe reduction in Alk Phos activity was observed after day 14, while control $Dicer^{c/c}$ calvarial cells reached peak levels in activity and mRNA (Fig. 4B, C). Significantly, $Dicer^{\Delta oc/\Delta oc}$ cells showed no induction of *Runx2* and *Osterix*, two transcription factors essential for further differentiation. In contrast, expression of *Col1a1*, the major bone protein was upregulated in Dicer ablated cells (Fig. 4C), consistent with the decrease in let-7a (Fig. 4C) which targets collagens (Li et al., 2009). A block in osteoblast differentiation occurs at the mineralization stage as reflected by lack of *OC* expression after day 14 (Fig. 4C). All the markers except *Col1a1* were at normal levels in proliferating cells, when *OC* promoter activity driving Cre expression is at low basal levels. These findings are analogous to ex vivo excision of $Dicer^{c/c}$ BMSCs (Fig. 2). Thus, mechanisms controlled by Dicer in mature osteoblasts support post-transcriptional regulation of target genes through miRs that are essential for mineralization of the bone ECM. Such targets would include well-characterized enzymes and matrix proteins (Li et al., 2009).

Dicer excision in mature osteoblasts/osteocytes increases bone mass in adult mice

Mice after birth were continuously monitored up to 8 mos and exhibited similar growth rates (data not shown). Unlike the severe defects observed at late gestation in $Dicer^{\Delta oc/\Delta oc}$ mice, radiography revealed that bone formation after birth (post-natal day 2 and 4 wk age) was normal (data not shown). However, at 2 mos of age increased radio-opacity was observed in femurs, spine and tail vertebrae in $Dicer^{\Delta oc/\Delta oc}$ compared of the $Dicer^{c/c}$ mice by (Supplementary Fig. S2). Cortical bone width increased and trabecular bone of the vertebrae became very dense. Interestingly, no differences could be observed in radiographs of calvarial bones at 2 mo of age between $Dicer^{\Delta oc/\Delta oc}$ and $Dicer^{c/c}$ mice (Supplementary Fig. S2). Hence, calvariae were not characterized further by μCT for detailed analyses.

At 1, 2, 4 and 8 mo of age, cortical and trabecular bone structure of femurs were evaluated by μCT analysis (Fig. 5). Single sagittal sections show increasing trabecular thickness (Fig. 5A)

and widened cortex (Fig. 5C) from 2 to 8 mo in $Dicer^{\Delta oc/\Delta oc}$ compared to $Dicer^{c/c}$. The trabeculae bone volume (BV/TV) indicates at 1 mo age, an 11.4% significant decrease compared to controls (Fig. 5B), but at 2 mo BV/TV was not significantly different. At 2 mo, trabecular parameters were beginning to change and during the next 2 mo of growth, a 5-fold increase in BV/TV was observed. Quantitative parameters specific for trabecular bone showed significant increases in the thickness (53%) and number (25%) in $Dicer^{\Delta oc/\Delta oc}$ at 4 mo and consistent with other parameters (Fig. 5B and Supplementary Fig. S3A).

Evidence of increased cortical bone mass was found earlier at 1 mo in $Dicer^{\Delta oc/\Delta oc}$ (29% higher cortical bone area) with decreased cortical porosity through 4 mo, although not significantly changed from $Dicer^{c/c}$ at 8 mo age (Fig. 5C, D). Other cortical parameters reflected maintenance of high bone mass in the cortex (Supplemental Fig. S4). Notably the periosteal area was more active than the endosteal surface of the cortex in $Dicer^{\Delta oc/\Delta oc}$ (Supplemental Fig. 4S) which accounted for normal marrow space. However, at 8 mo the endocortical surface had a greater response in contributing to bone formation than at earlier ages (Supplemental Fig. S4). Overall, at 8 mo when the control $Dicer^{c/c}$ mice have decreased trabecular and cortical bone mass, $Dicer^{\Delta oc/\Delta oc}$ continued to accumulate cortical bone from 4 to 8 mos (Fig. 5C).

In summary, the delayed bone formation phenotype observed in $Dicer^{\Delta oc/\Delta oc}$ neonates was resolved during post-natal growth and resolved at puberty age (8 wk). This reversal of the phenotype documented in long bone, lumbar and tail vertebrae is well underway from 1–2 mo, stabilized by 4 mo and continues to increase bone mass up to 8 mo in $Dicer^{\Delta oc/\Delta oc}$. Although a significantly higher accumulation of bone tissue formed by the endochondral process of bone formation and the periosteal surface of long bone, membranous calvarial bone was spared from excessive bone formation.

Increased bone mass is represented by normal cellular and tissue organization

To identify the possible changes in cellular organization of bone tissue caused by high bone mass phenotype in absence of Dicer in mature osteoblasts, we performed histological and molecular studies of the femurs at 2 mo age $Dicer^{c/c}$ and $Dicer^{\Delta oc/\Delta oc}$ mice when the phenotype is reversed. The Toluidine blue stained sections of cortical bone (femur mid-shaft region shown in Fig. 6A, left panels) reveals individual osteocytes in their lacunae with blood vessel channels throughout in both groups, but thicker bone in $Dicer^{\Delta oc/\Delta oc}$ mice which appears to have 3 zones of accumulated bone. The most mature bone (deposited from birth), which takes up less Toluidine blue stain, is on the endosteal surface, while the middle zone represents bone accumulated during rapid post-natal growth and is seen as vascularized. The third layer of recently laid down bone formed from the periosteal surface has rows of osteocytes in individual lacunae with fewer blood vessel channels. This organization of new growth more from the periosteum is supported by μCT parameters (Supplemental Fig. S4). Histomorphometric quantitation of osteocytes in the cortical bone (n= 4 fields of bone along the cortex in n =3 mice) indicates that while the total number of osteocytes is 2-fold (data not shown) higher because of increased bone volume, the osteocyte density per unit area is similar in $Dicer^{c/c}$ and $Dicer^{\Delta oc/\Delta oc}$ (Fig. 6A, right panel).

We had previously identified (Li *et al.*, 2009) that a significant number of microRNAs are upregulated from days 21 to 28, the mineralization stage when the ECM is mineralized and cells are transitioned from osteoblast to osteocytes in MC3T3 cells (Sudo et al., 1983). At least 6 upregulated microRNAs, based on bioinformatic studies, target collagen type I that constitutes greater than 90% of adult bone ECM. Therefore we tested the hypothesis that a contributing mechanism to the observed phenotype is a stimulated production of type I collagen that accelerated the transition to osteocytes. Total cellular RNA was prepared from long bone flushed of marrow at 4 mo when the phenotype of $Dicer^{\Delta oc/\Delta oc}$ was fully developed. Q-PCR analyses of multiple collagen transcripts at 4-mo of age revealed that the expression of bone-

specific collagens (Col1a1, Col1a2 and Col5) were upregulated; whereas Col3a1, known to be expressed in immature bone, is at low and equivalent levels in $Dicer^{\Delta oc/\Delta oc}$ and $Dicer^{c/c}$ mice (Fig. 6B), indicating an involvement of collagen proteins as part of the mechanism for high bone mass in $Dicer^{\Delta oc/\Delta oc}$ mice. Although the Run×2 transcription was not significantly different between the two groups, reflecting that commitment to the osteoblast lineage is not enhanced, the Osterix transcriptional regulator of later differentiation and osteocalcin reflecting a mineralized matrix are increased by <30% in $Dicer^{\Delta oc/\Delta oc}$ mice. We also examined expression of *Sclerostin* mRNA levels, a specific product of osteocytes that is an inhibitor of Wnt signaling positive effects on bone formation (ten et al., 2008). However, we find no statistical difference between $Dicer^{c/c}$ and $Dicer^{\Delta oc/\Delta oc}$ mice (data not shown), further indicating that osteocyte function is normal.

Several high bone mass (HBM) mouse models, such as the LRP5 activating mutation and Sclerostin null mice display an uncoupling of bone turnover which leads to increased bone tissue deposition (Babij et al., 2003; Li et al., 2008a). To examine this possibility in $Dicer^{\Delta oc/\Delta oc}$ mice, osteoclast-specific tartrate resistant acid phosphatase (TRAP) staining was performed on bone sections from 2 mo-old mice (Fig. 6C). Overall, there is an increase in the number of osteoblasts in the metaphyses because there is an increase in bone trabecular surfaces. This finding suggests that bone remodeling is coupled to ensure resorption of calcified cartilage in the primary spongiosa and conversion to lamellar from newly secreted woven bone. Furthermore, increased osteoclasts are observed in cutting cones in cortical bone of $Dicer^{\Delta oc/\Delta oc}$ mice to vascularize the thickened tissue (Fig. 6D). Consistent with these observations, the mRNA levels of TRAP (originating from osteoclast) and RANKL, the osteoblast coupling factor for osteoclast differentiation, were both upregulated in bone tissues from $Dicer^{\Delta oc/\Delta oc}$ mice (Fig. 6E). These findings indicate that the phenotype of $Dicer^{\Delta oc/\Delta oc}$ mice is not because of a reduction in bone resorption. Rather, a coupling of increased bone remodeling to increased bone formation is revealed.

DISCUSSION

Control of mesenchymal differentiation is an intricate process requiring the interplay of cell signaling, transcription, and post-transcriptional mechanisms. Our studies now show that miR-mediated control of gene expression is critical for osteogenesis and bone homeostasis. These findings are based on several key findings that establish functions of Dicer in bone tissue. First, we have identified the Dicer enzyme as essential for membranous and endochondral bone formation in mid-stage embryos (E14.5). Second, deletion of *Dicer* by *OC*-Cre in mature osteoblasts delayed bone formation before birth. However, this phenotype was reversed post-natally and adult mice showed a dramatic increase in bone mass compared to controls. Third, in the $Dicer^{\Delta oc/\Delta oc}$ post-natal skeleton a continual accrual of trabecular and cortical bone occurs up to age 8 mos with normal bone remodeling such that the thickened tissue is vascularized. Fourth, ex vivo studies indicate that the cellular mechanisms which are impaired by Dicer deletion in osteoprogenitor cells are related to post-proliferative differentiation of committed osteoblasts. We conclude from these observations that Dicer function is rate-limiting for the processing of specific miRs at distinct developmental stages of bone tissue formation in long bones and vertebral bodies. In summary, our findings suggest that Dicer processes a distinct set of miRs in the fetal skeleton necessary for osteogenesis, whereas in the adult skeleton miRs present in mature osteoblasts are potent negative regulators of excessive bone formation. Thus, Dicer produced mature miRs in osteoblast lineage cells have potent activities in regulating cell determination, differentiation and tissue homeostasis and exhibit a specificity for specific anatomical bone tissues.

Mechanisms contributing to the phenotype of delayed osteoblast differentiation before birth were revealed by ex vivo characterization of defective cell differentiation along the osteoblast

lineage. We find that the critical stage for which miRs are required in mesenchymal cells occurs early in the osteoblast maturation sequence, shortly after commitment to the osteoblast lineage. Neonatal calvarial cells from $Dicer^{\Delta oc/\Delta oc}$ exhibited a block in osteoblast maturation, consistent with in vitro Dicer-ablated bone marrow derived osteoprogenitors from $Dicer^{c/c}$ mice. In both cell models, Run×2 was found at equivalent levels prior to differentiation; and, proliferation and multi-layering of cells are not compromised, as Alk Phos positive bone nodules are present throughout the culture. However, the nodules are defective in their ability to mineralize, in part compromised by further induction of Alk Phos and absence of non-collagenous proteins (bone sialoprotein and osteocalcin) that are normally induced in post-proliferative osteoblasts to support mineralization of the bone ECM (Alford and Hankenson, 2006; Malaval et al., 2008; Robey and Boskey, 2008). These findings suggest that a critical set of miRs must be expressed in post-proliferative osteoblasts to indirectly activate bone-related proteins required to produce a mineralizing ECM.

While inhibition of osteoblast differentiation is similar in *ex vivo* cultured cells from our two mouse models, the striking differences in the *in vivo* phenotypes can be explained by the distinct expression patterns of the promoters used in our studies. The *Col1a1* promoter is active in preosteoblasts, the inner cell layer of the periosteum that will become a bone collar (Liu et al., 2004). Thus, Dicer ablation by *Col1a1*-Cre between E14.5 and E15.5, when there is a rapid induction of mineralizing elements in control mice, compromises differentiation of osteoprogenitor cells exhibiting Dicer loss-of-function. *Osteocalcin*-Cre mice are well documented for robust activity in the post-natal mouse (Chiang *et al.*, 2009; Yuan *et al.*, 2008). There are distinct differences between the pre- and post-natal bone phenotype in the $Dicer^{\Delta oc/\Delta oc}$ mice. Before birth, bone formation is delayed, and ex vivo osteoprogenitor cells from these mice exhibit a similar phenotype as ex vivo Dicer excision of bone marrow mesenchymal cells, both defective in differentiation to mature osteoblasts. The histology of bone from E17.5 shows few mature osteoblasts, and suggests that the immature cells expressing low basal *osteocalcin* may have different functioning miRs than those expressed in mature osteoblasts in a mineralized matrix after birth. In contrast, adult mice showed increased bone accumulation in the appendicular skeleton and spine, and with a normal cellular organization.

A high bone mass phenotype in $Dicer^{\Delta oc/\Delta oc}$ was evident after weaning initially in tail vertebrae and cortical bone. At 4 weeks age, cortical bone in $Dicer^{\Delta oc/\Delta oc}$ increases prior to trabecular which becomes normal relative to $Dicer^{c/c}$. This phenotype of decreased trabecular bone, but increased cortical bone has been observed in other mouse models where cortical bone compensates for weak structure of trabecular bone (Morko et al., 2005; Turner et al., 2000). However, beyond 2 months, a high bone mass phenotype was clearly established which included cortical and trabecular bone of limbs and vertebrae. Notably, the calvarium is not affected. It is possible that excessive growth of calvarial bone may be regulated by mechanisms other than through miRNAs which limit the size of other bones in the body.

A striking feature of the increased bone mass of the limbs was stimulation of newly formed bone from 1 month to after 4 months of age occurring largely from the periosteal surfaced and more on the lateral than the medial side of the limb. This observation suggests two contributing mechanistic pathways that are likely to be influenced by miRNA regulation. First, the bone extracellular matrix harbors numerous growth factors, which contribute to both proliferative expansion of pre-osteoblasts and their differentiation e.g. IGF-1, FGFs, BMPs and TGFβ, which have been well studied (reviewed in (Allori et al., 2008; Giustina et al., 2008; Ornitz, 2005). Any increase in their levels could potentially stimulate bone formation. Secondly, the finding of a more profound effect on long bone indicates that mechanical forces on the bone may in part be contributing to the stimulated bone formation as the periosteum is well documented for its responses to mechanical stimulation and tissue repair (Henriksen et al., 2009). Furthermore, osteocytes are the responsive “mechanotransducer cells” of bones

(reviewed in (Bonewald and Johnson, 2008)), which can secrete factors to stimulate the activity of the surface osteoblast (Bonewald *et al.*, 2008; Heino et al., 2004; Hirao et al., 2007). The osteocytes are organized in individual lacunae at a density equivalent to control. Further, bone remodeling and osteoclast activity is not impaired and the thickened bone becomes vascularized to maintain viability of the osteocytes.

Insight into the mechanisms for the Dicer$^{\Delta oc/\Delta oc}$ post-natal phenotype of increased bone mass is obtained from our recent profiling studies of miRs during osteoblast differentiation. We identified a large representation of miRs during the mineralization period which target collagens and proved miR-29b directly downregulated four different collagens (Li et al., 2009). After birth, resolution of the initial delay in bone formation followed by continuous increase in bone mass in Dicer$^{\Delta oc/\Delta oc}$ adult mice may be due to loss of miRs that target bone matrix extracellular proteins. For example, we confirmed in the present studies loss of let-7a and miR-29b and following Dicer excision in osteoblasts and with concomitant increases in collagen levels in bone of the Dicer$^{\Delta oc/\Delta oc}$ mice, including the major protein of the bone ECM (90% type I collagen). Establishment of a collagen scaffold promotes osteoblast differentiation and mineralization (Franceschi et al., 1994; Lynch et al., 1995). In the absence of Dicer, miRs that inhibit biosynthesis of matrix proteins are not processed, and consequently bone formation can progress unimpeded to produce a greater than 2-fold increase in bone volume by 4 months that is retained up to 8 months. The process driving osteoblasts to osteocyte maturation may arise from stimulated secretion of ECM that accelerates the enveloping of surface osteoblasts to further differentiate (Bonewald *et al.*, 2008). Thus, while the Dicer enzyme is essential in early osteoprogenitors for bone formation, excision of *Dicer* has an anabolic effect on the adult skeleton due to loss of miRs that are required to regulate bone mass.

In conclusion, our findings have now identified functions for Dicer during development of the osteoblast phenotype for tissue morphogenesis and for post-natal regulation of bone accrual. These findings provide a potential approach for stimulating bone formation with antagomirs upon identification of the specific microRNAs contributing to the anabolic phenotype in adult bone.

Supplementary Material

Refer to Web version on PubMed Central for supplementary material.

Acknowledgments

This work was supported by NIH grants R01AR039588 (GSS), P01AR048818 (GSS), R37DE012528 (JBL), DK73324 (SNJ), CA77735 (SNJ), DK032520 (for Core facilities), and S10RR023540 from the National Center for Research Resources (JBL). RM was supported in part by an American Heart Award (0625823T) and by NIH-T32CA130807. The contents of this manuscript are solely the responsibility of the authors and do not necessarily represent the official views of the National Center for Research Resources or the National Institutes of Health.

References

Alford AI, Hankenson KD. Matricellular proteins: Extracellular modulators of bone development, remodeling, and regeneration. Bone 2006;38:749–757. [PubMed: 16412713]

Allori AC, Sailon AM, Warren SM. Biological basis of bone formation, remodeling, and repair-part I: biochemical signaling molecules. Tissue Eng Part B Rev 2008;14:259–273. [PubMed: 18665803]

Andl T, Murchison EP, Liu F, Zhang Y, Yunta-Gonzalez M, Tobias JW, Andl CD, Seykora JT, Hannon GJ, Millar SE. The miRNA-processing enzyme dicer is essential for the morphogenesis and maintenance of hair follicles. Curr Biol 2006;16:1041–1049. [PubMed: 16682203]

Babij P, Zhao W, Small C, Kharode Y, Yaworsky PJ, Bouxsein ML, Reddy PS, Bodine PV, Robinson JA, Bhat B, Marzolf J, Moran RA, Bex F. High bone mass in mice expressing a mutant LRP5 gene. J Bone Miner Res 2003;18:960–974. [PubMed: 12817748]

Bernstein E, Kim SY, Carmell MA, Murchison EP, Alcorn H, Li MZ, Mills AA, Elledge SJ, Anderson KV, Hannon GJ. Dicer is essential for mouse development. Nat Genet 2003;35:215–217. [PubMed: 14528307]

Blakaj A, Lin H. Piecing together the mosaic of early mammalian development through microRNAs. J Biol Chem 2008;283:9505–9508. [PubMed: 18272516]

Bonewald LF, Johnson ML. Osteocytes, mechanosensing and Wnt signaling. Bone 2008;42:606–615. [PubMed: 18280232]

Chen JF, Murchison EP, Tang R, Callis TE, Tatsuguchi M, Deng Z, Rojas M, Hammond SM, Schneider MD, Selzman CH, Meissner G, Patterson C, Hannon GJ, Wang DZ. Targeted deletion of Dicer in the heart leads to dilated cardiomyopathy and heart failure. Proc Natl Acad Sci U S A 2008;105:2111–2116. [PubMed: 18256189]

Chiang C, Chiu WM, Moore AJ, Anderson PH, Ghasem-Zadeh A, McManus JF, Ma C, Seeman E, Clemens TL, Morris HA, Zajac JD, Davey RA. Mineralization and bone resorption are regulated by the androgen receptor in male mice. J Bone Miner Res 2009;24:621–631. [PubMed: 19049333]

Cobb BS, Nesterova TB, Thompson E, Hertweck A, O'Connor E, Godwin J, Wilson CB, Brockdorff N, Fisher AG, Smale ST, Merkenschlager M. T cell lineage choice and differentiation in the absence of the RNase III enzyme Dicer. J Exp Med 2005;201:1367–1373. [PubMed: 15867090]

da Costa Martins PA, Bourajjaj M, Gladka M, Kortland M, van Oort RJ, Pinto YM, Molkentin JD, De Windt LJ. Conditional dicer gene deletion in the postnatal myocardium provokes spontaneous cardiac remodeling. Circulation 2008;118:1567–1576. [PubMed: 18809798]

Damiani D, Alexander JJ, O'Rourke JR, McManus M, Jadhav AP, Cepko CL, Hauswirth WW, Harfe BD, Strettoi E. *Dicer* inactivation leads to progressive functional and structural degeneration of the mouse retina. J Neurosci 2008;28:4878–4887. [PubMed: 18463241]

Davis TH, Cuellar TL, Koch SM, Barker AJ, Harfe BD, McManus MT, Ullian EM. Conditional loss of Dicer disrupts cellular and tissue morphogenesis in the cortex and hippocampus. J Neurosci 2008;28:4322–4330. [PubMed: 18434510]

Dimri GP, Lee X, Basile G, Acosta M, Scott G, Roskelley C, Medrano EE, Linskens M, Rubelj I, Pereira-Smith O. A biomarker that identifies senescent human cells in culture and in aging skin in vivo. Proc Natl Acad Sci U S A 1995;92:9363–9367. [PubMed: 7568133]

Franceschi RT, Iyer BS, Cui Y. Effects of ascorbic acid on collagen matrix formation and osteoblast differentiation in murine MC3T3-E1 cells. J Bone Miner Res 1994;9:843–854. [PubMed: 8079660]

Giustina A, Mazziotti G, Canalis E. Growth hormone, insulin-like growth factors, and the skeleton. Endocr Rev 2008;29:535–559. [PubMed: 18436706]

Harfe BD, McManus MT, Mansfield JH, Hornstein E, Tabin CJ. The RNaseIII enzyme Dicer is required for morphogenesis but not patterning of the vertebrate limb. Proc Natl Acad Sci U S A 2005;102:10898–10903. [PubMed: 16040801]

Harris KS, Zhang Z, McManus MT, Harfe BD, Sun X. Dicer function is essential for lung epithelium morphogenesis. Proc Natl Acad Sci U S A 2006;103:2208–2213. [PubMed: 16452165]

Harvey SJ, Jarad G, Cunningham J, Goldberg S, Schermer B, Harfe BD, McManus MT, Benzing T, Miner JH. Podocyte-specific deletion of dicer alters cytoskeletal dynamics and causes glomerular disease. J Am Soc Nephrol 2008;19:2150–2158. [PubMed: 18776121]

Hayashi K, Chuva de Sousa Lopes SM, Kaneda M, Tang F, Hajkova P, Lao K, O'Carroll D, Das PP, Tarakhovsky A, Miska EA, Surani MA. MicroRNA biogenesis is required for mouse primordial germ cell development and spermatogenesis. PLoS ONE 2008;3:e1738. [PubMed: 18320056]

Heino TJ, Hentunen TA, Vaananen HK. Conditioned medium from osteocytes stimulates the proliferation of bone marrow mesenchymal stem cells and their differentiation into osteoblasts. Exp Cell Res 2004;294:458–468. [PubMed: 15023534]

Henriksen K, Neutzsky-Wulff AV, Bonewald LF, Karsdal MA. Local communication on and within bone controls bone remodeling. Bone 2009;44:1026–1033. [PubMed: 19345750]

Hirao M, Hashimoto J, Yamasaki N, Ando W, Tsuboi H, Myoui A, Yoshikawa H. Oxygen tension is an important mediator of the transformation of osteoblasts to osteocytes. J Bone Miner Metab 2007;25:266–276. [PubMed: 17704991]

Jaskiewicz L, Filipowicz W. Role of Dicer in posttranscriptional RNA silencing. Curr Top Microbiol Immunol 2008;320:77–97. [PubMed: 18268840]

Kanellopoulou C, Muljo SA, Kung AL, Ganesan S, Drapkin R, Jenuwein T, Livingston DM, Rajewsky K. Dicer-deficient mouse embryonic stem cells are defective in differentiation and centromeric silencing. Genes Dev 2005;19:489–501. [PubMed: 15713842]

Kobayashi T, Lu J, Cobb BS, Rodda SJ, McMahon AP, Schipani E, Merkenschlager M, Kronenberg HM. Dicer-dependent pathways regulate chondrocyte proliferation and differentiation. Proc Natl Acad Sci U S A 2008;105:1949–1954. [PubMed: 18238902]

Koralov SB, Muljo SA, Galler GR, Krek A, Chakraborty T, Kanellopoulou C, Jensen K, Cobb BS, Merkenschlager M, Rajewsky N, Rajewsky K. Dicer ablation affects antibody diversity and cell survival in the B lymphocyte lineage. Cell 2008;132:860–874. [PubMed: 18329371]

Lengner CJ, Lepper C, van Wijnen AJ, Stein JL, Stein GS, Lian JB. Primary mouse embyronic fibroblasts: a model of mesenchymal cartilage formation. J Cell Physiol 2004;200:327–333. [PubMed: 15254959]

Li X, Ominsky MS, Niu QT, Sun N, Daugherty B, D'Agostin D, Kurahara C, Gao Y, Cao J, Gong J, Asuncion F, Barrero M, Warmington K, Dwyer D, Stolina M, Morony S, Sarosi I, Kostenuik PJ, Lacey DL, Simonet WS, Ke HZ, Paszty C. Targeted deletion of the sclerostin gene in mice results in increased bone formation and bone strength. J Bone Miner Res 2008a;23:860–869. [PubMed: 18269310]

Li Z, Hassan MQ, Jafferji M, Garzon R, Croce CM, van Wijnen AJ, Stein JL, Stein GS, Lian JB. Biological functions of miR-29b contribute to positive regulation of osteoblast differentiation. J Biol Chem 2009;284:15676–15684. [PubMed: 19342382]

Li Z, Hassan MQ, Volinia S, van Wijnen AJ, Stein JL, Croce CM, Lian JB, Stein GS. A microRNA signature for a BMP2-induced osteoblast lineage commitment program. Proc Natl Acad Sci USA 2008b;105:13906–13911. [PubMed: 18784367]

Lian JB, Stein GS, Javed A, van Wijnen AJ, Stein JL, Montecino M, Hassan MQ, Gaur T, Lengner CJ, Young DW. Networks and hubs for the transcriptional control of osteoblastogenesis. Rev Endocr Metab Disord 2006;7:1–16. [PubMed: 17051438]

Liu F, Woitge HW, Braut A, Kronenberg MS, Lichtler AC, Mina M, Kream BE. Expression and activity of osteoblast-targeted Cre recombinase transgenes in murine skeletal tissues. Int J Dev Biol 2004;48:645–653. [PubMed: 15470637]

Lufkin T, Mark M, Hart CP, Dolle P, LeMeur M, Chambon P. Homeotic transformation of the occipital bones of the skull by ectopic expression of a homeobox gene. Nature 1992;359:835–841. [PubMed: 1359423]

Luzi E, Marini F, Sala SC, Tognarini I, Galli G, Brandi ML. Osteogenic differentiation of human adipose tissue-derived stem cells is modulated by the miR-26a targeting of the SMAD1 transcription factor. J Bone Miner Res 2008;23:287–295. [PubMed: 18197755]

Lynch MP, Stein JL, Stein GS, Lian JB. The influence of type I collagen on the development and maintenance of the osteoblast phenotype in primary and passaged rat calvarial osteoblasts: modification of expression of genes supporting cell growth, adhesion, and extracellular matrix mineralization. Exp Cell Res 1995;216:35–45. [PubMed: 7813631]

Malaval L, Wade-Gueye NM, Boudiffa M, Fei J, Zirngibl R, Chen F, Laroche N, Roux JP, Burt-Pichat B, Duboeuf F, Boivin G, Jurdic P, Lafage-Proust MH, Amedee J, Vico L, Rossant J, Aubin JE. Bone sialoprotein plays a functional role in bone formation and osteoclastogenesis. J Exp Med 2008;205:1145–1153. [PubMed: 18458111]

Miao D, Scutt A. Histochemical localization of alkaline phosphatase activity in decalcified bone and cartilage. J Histochem Cytochem 2002;50:333–340. [PubMed: 11850436]

Mizuno Y, Yagi K, Tokuzawa Y, Kanesaki-Yatsuka Y, Suda T, Katagiri T, Fukuda T, Maruyama M, Okuda A, Amemiya T, Kondoh Y, Tashiro H, Okazaki Y. miR-125b inhibits osteoblastic differentiation by down-regulation of cell proliferation. Biochem Biophys Res Commun 2008a; 368:267–272. [PubMed: 18230348]

Mizuno Y, Yagi K, Tokuzawa Y, Kanesaki-Yatsuka Y, Suda T, Katagiri T, Fukuda T, Maruyama M, Okuda A, Amemiya T, Kondoh Y, Tashiro H, Okazaki Y. miR-125b inhibits osteoblastic differentiation by down-regulation of cell proliferation. Biochem Biophys Res Commun 2008b; 368:267–272. [PubMed: 18230348]

Morko J, Kiviranta R, Hurme S, Rantakokko J, Vuorio E. Differential turnover of cortical and trabecular bone in transgenic mice overexpressing cathepsin K. Bone 2005;36:854–865. [PubMed: 15826870]

Mudhasani R, Zhu Z, Hutvagner G, Eischen CM, Lyle S, Hall LL, Lawrence JB, Imbalzano AN, Jones SN. Loss of miRNA biogenesis induces p19Arf-p53 signaling and senescence in primary cells. J Cell Biol 2008;181:1055–1063. [PubMed: 18591425]

Muljo SA, Ansel KM, Kanellopoulou C, Livingston DM, Rao A, Rajewsky K. Aberrant T cell differentiation in the absence of Dicer. J Exp Med 2005;202:261–269. [PubMed: 16009718]

Murchison EP, Stein P, Xuan Z, Pan H, Zhang MQ, Schultz RM, Hannon GJ. Critical roles for Dicer in the female germline. Genes Dev 2007;21:682–693. [PubMed: 17369401]

Nagaraja AK, Andreu-Vieyra C, Franco HL, Ma L, Chen R, Han DY, Zhu H, Agno JE, Gunaratne PH, DeMayo FJ, Matzuk MM. Deletion of Dicer in somatic cells of the female reproductive tract causes sterility. Mol Endocrinol 2008;22:2336–2352. [PubMed: 18687735]

Nakasa T, Miyaki S, Okubo A, Hashimoto M, Nishida K, Ochi M, Asahara H. Expression of microRNA-146 in rheumatoid arthritis synovial tissue. Arthritis Rheum 2008;58:1284–1292. [PubMed: 18438844]

O'Rourke JR, Georges SA, Seay HR, Tapscott SJ, McManus MT, Goldhamer DJ, Swanson MS, Harfe BD. Essential role for Dicer during skeletal muscle development. Dev Biol 2007;311:359–368. [PubMed: 17936265]

Ornitz DM. FGF signaling in the developing endochondral skeleton. Cytokine Growth Factor Rev 2005;16:205–213. [PubMed: 15863035]

Oskowitz AZ, Lu J, Penfornis P, Ylostalo J, McBride J, Flemington EK, Prockop DJ, Pochampally R. Human multipotent stromal cells from bone marrow and microRNA: regulation of differentiation and leukemia inhibitory factor expression. Proc Natl Acad Sci U S A 2008;105:18372–18377. [PubMed: 19011087]

Pratap J, Galindo M, Zaidi SK, Vradii D, Bhat BM, Robinson JA, Choi JY, Komori T, Stein JL, Lian JB, Stein GS, van Wijnen AJ. Cell growth regulatory role of Run×2 during proliferative expansion of pre-osteoblasts. Cancer Res 2003;63:5357–5362. [PubMed: 14500368]

Robey, PG.; Boskey, AL. The composition of bone. In: Rosen, CJ., editor. Primer on the Metabolic Bone Diseases and Disorders of Mineral Metabolism. American Society for Bone and Mineral Research; Washington, DC: 2008. p. 32-38.

Schaefer A, O'Carroll D, Tan CL, Hillman D, Sugimori M, Llinas R, Greengard P. Cerebellar neurodegeneration in the absence of microRNAs. J Exp Med 2007;204:1553–1558. [PubMed: 17606634]

Serrano M, Lee H, Chin L, Cordon-Cardo C, Beach D, DePinho RA. Role of the INK4a locus in tumor suppression and cell mortality. Cell 1996;85:27–37. [PubMed: 8620534]

Soltanoff CS, Yang S, Chen W, Li YP. Signaling networks that control the lineage commitment and differentiation of bone cells. Crit Rev Eukaryot Gene Expr 2009;19:1–46. [PubMed: 19191755]

Sudo H, Kodama HA, Amagai Y, Yamamoto S, Kasai S. In vitro differentiation and calcification in a new clonal osteogenic cell line derived from newborn mouse calvaria. J Cell Biol 1983;96:191–198. [PubMed: 6826647]

Sugatani T, Hruska KA. Impaired micro-RNA pathways diminish osteoclast differentiation and function. J Biol Chem 2009;284:4667–4678. [PubMed: 19059913]

ten DP, Krause C, de Gorter DJ, Lowik CW, Van Bezooijen RL. Osteocyte-derived sclerostin inhibits bone formation: its role in bone morphogenetic protein and Wnt signaling. J Bone Joint Surg Am 2008;90(Suppl 1):31–35.

Tuddenham L, Wheeler G, Ntounia-Fousara S, Waters J, Hajihosseini MK, Clark I, Dalmay T. The cartilage specific microRNA-140 targets histone deacetylase 4 in mouse cells. FEBS Lett 2006;580:4214–4217. [PubMed: 16828749]

Turner CH, Hsieh YF, Muller R, Bouxsein ML, Baylink DJ, Rosen CJ, Grynpas MD, Donahue LR, Beamer WG. Genetic regulation of cortical and trabecular bone strength and microstructure in inbred strains of mice. J Bone Miner Res 2000;15:1126–1131. [PubMed: 10841181]

Yang WJ, Yang DD, Na S, Sandusky GE, Zhang Q, Zhao G. Dicer is required for embryonic angiogenesis during mouse development. J Biol Chem 2005;280:9330–9335. [PubMed: 15613470]

Yi R, O'Carroll D, Pasolli HA, Zhang Z, Dietrich FS, Tarakhovsky A, Fuchs E. Morphogenesis in skin is governed by discrete sets of differentially expressed microRNAs. Nat Genet 2006;38:356–362. [PubMed: 16462742]

Yuan B, Takaiwa M, Clemens TL, Feng JQ, Kumar R, Rowe PS, Xie Y, Drezner MK. Aberrant Phex function in osteoblasts and osteocytes alone underlies murine X-linked hypophosphatemia. J Clin Invest 2008;118:722–734. [PubMed: 18172553]

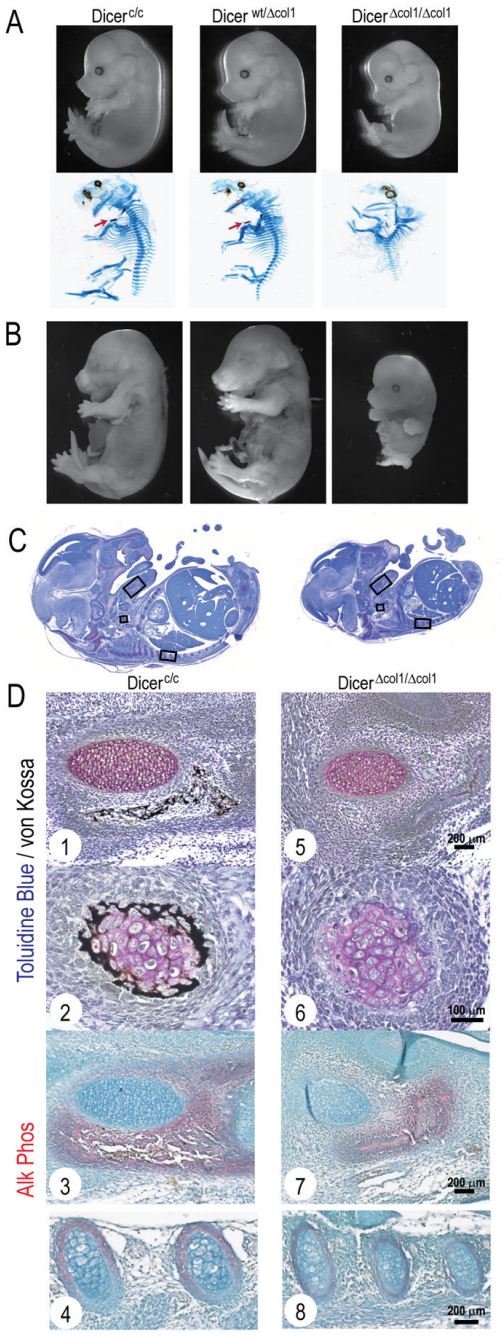

Figure 1. *In vivo* excision of *Dicer* by *Col1a1*-Cre impairs bone formation at E14.5 and induces embryonic lethality

(A) Skeletal deformities observed at E14.5. Upper panel shows smaller but viable $Dicer^{\Delta col1/\Delta col1}$ embryos at E14.5. Alcian Blue/Alizarin Red staining (lower panel) reveals lack of mineralizing clavicles (see arrow in $Dicer^{c/c}$ and $Dicer^{wt/\Delta col1}$) and a deformed cartilaginous skeleton in $Dicer^{\Delta col1/\Delta col1}$. (B) Images of E15.5 fetal pups show partial resorption of $Dicer^{\Delta col1/\Delta col1}$ pup. (C) Embryo sections are compared at E14.5 and (D) detailed (boxed areas) at higher magnification for $Dicer^{c/c}$ (1–4) and $Dicer^{\Delta col1/\Delta col1}$ (5–8), showing severely impaired mineralization of mandible mesenchyme that surrounds Meckel's cartilage

(1, 5), clavicle (2, 6) and reduced Alk Phos staining in the lower jaw (3, 7) and ribs (4, 8) of $Dicer^{\Delta col1/\Delta col1}$ embryos.

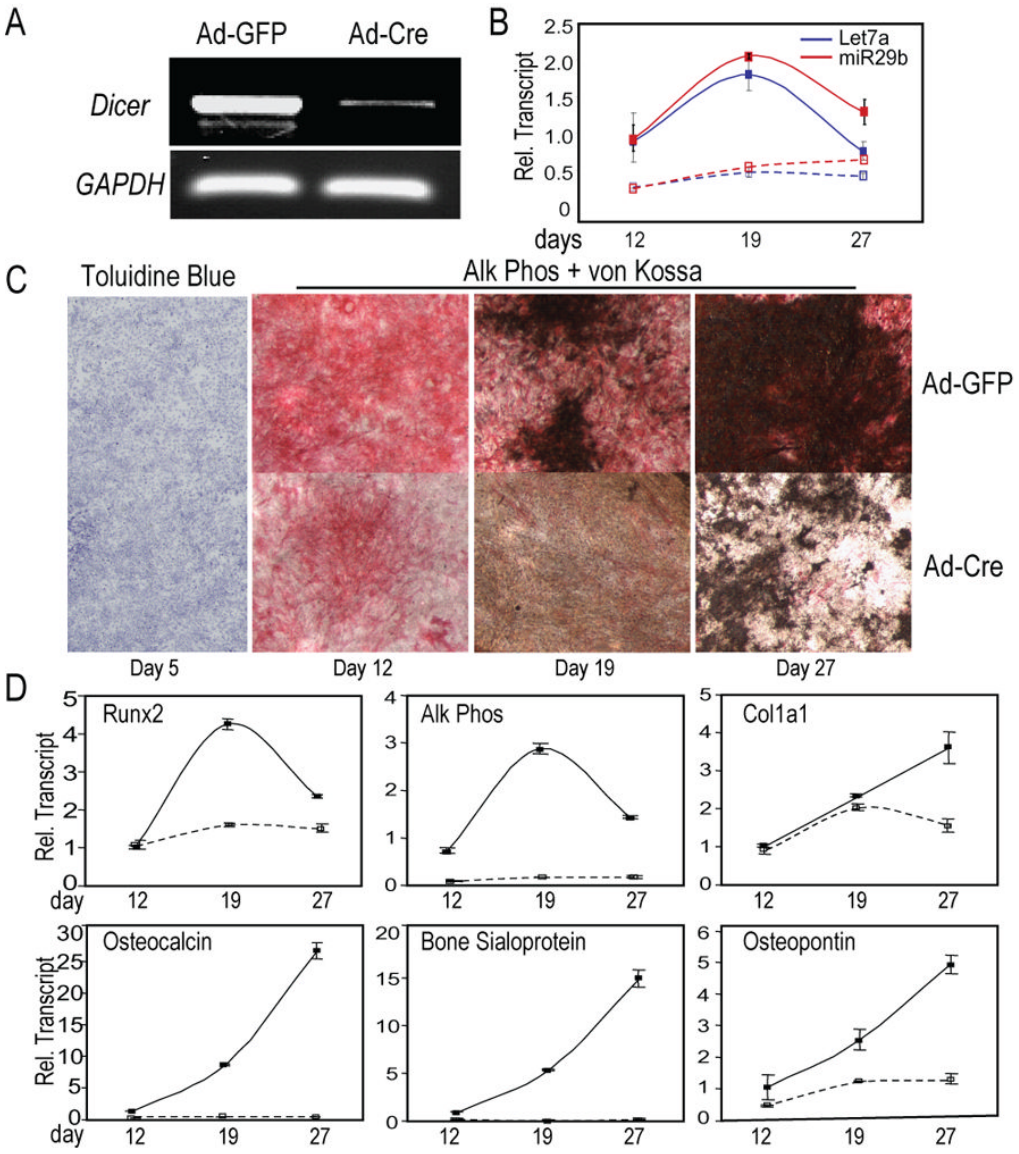

Figure 2. Contributing mechanisms for defective osteoblast differentiation in the absence of Dicer

Dicer excision in BMSCs from Dicer$^{c/c}$ mice by Ad-Cre, followed by differentiation into osteoblasts. Ad-GFP was used as control for infection of cells. (A) Genomic PCR of Ad-GFP (control) and Ad-Cre treated cells identified >90% excision of *Dicer* locus on day 5 (*GAPDH*, internal control). (B) Lack of miR-29b (Red lines) and let-7a (Blue lines) expression in the absence of Dicer. Solid lines (—) show control Ad-GFP treated cells; dotted lines (---), Ad-Cre Dicer-ablated cells. (C) Cellularity (Tol Blue) was not affected by *Dicer* excision, but differentiation (Alk Phos activity) and mineral (von Kossa stain) were severely impaired. (D) Expression patterns of early markers of committed osteoprogenitors, *Runx2* and *Col1a1*, and components for the onset and regulation of mineralization by the non-collagenous proteins, *OC*, *BSP* and *OP*, reflect impaired maturation of osteoblasts in *Dicer*-excised (Ad-Cre) cells.

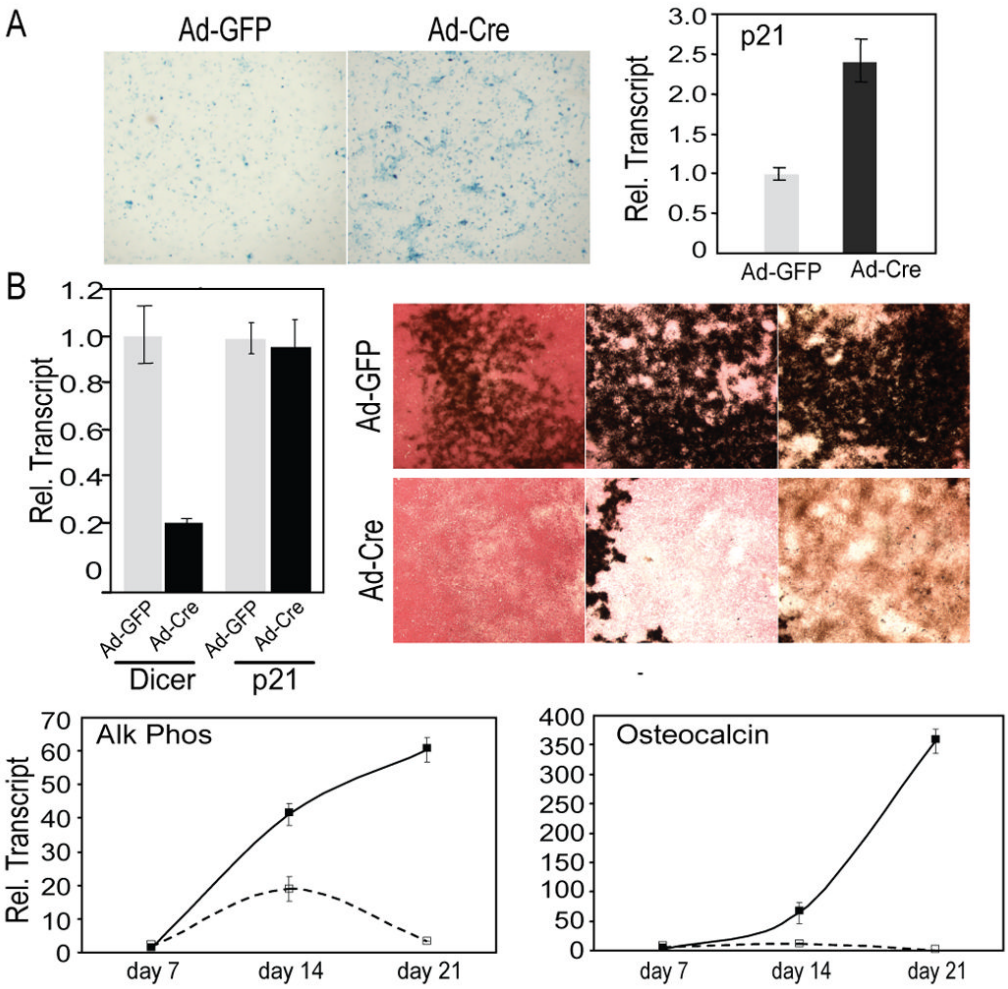

Figure 3. *Dicer* excision-induced defects in osteoblast differentiation occur in the cellular senescence-resistant Dicer$^{c/c}$; Ink4a/Arf$^{-/-}$ mice

(A) SA-βGal staining of control (Ad-GFP) or Dicer-ablated (Ad-Cre) BMSCs at day 5 shows increased senescence in the absence of Dicer. qRT-PCR analysis shows the cellular senescence marker p21. (B) BMSCs from Dicer$^{c/c}$; Ink4a/Arf$^{-/-}$ mice were transduced with Ad-Cre, and cultured for osteogenesis. qRT-PCR shows reduced *Dicer* mRNA after Ad-Cre-mediated excision, and p21 expression shows rescue of premature cell senescence in cells lacking Dicer. Alk Phos/von Kossa staining identifies reduced osteoblast differentiation from day 14 to 28 in absence of *Dicer*. qRT-PCR analysis of mRNAs at days 7–21. Solid lines (—) show control Ad-GFP treated cells; dotted lines (---), Ad-Cre Dicer-ablated cells. The data are presented as mean± SD, n=3.

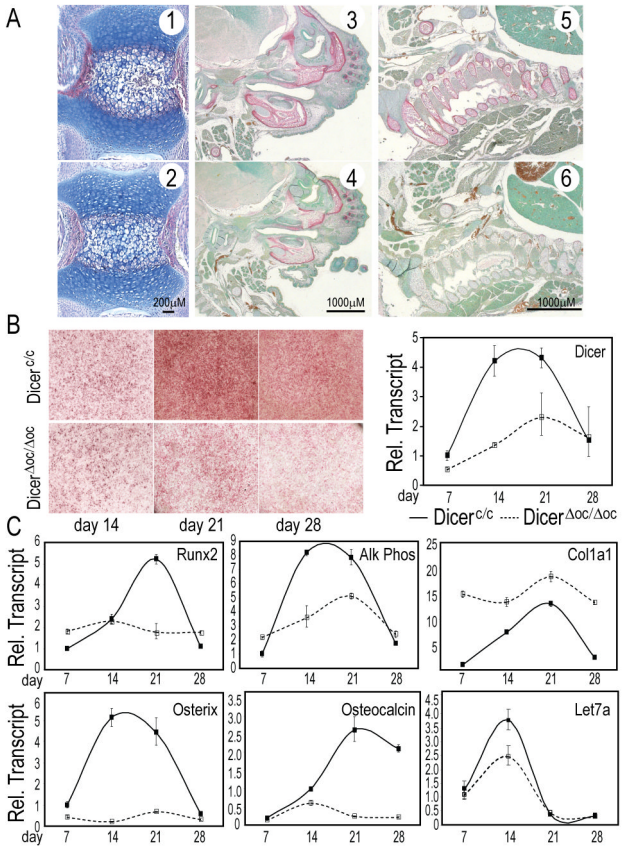

Figure 4. In vivo excision of *Dicer* by *OC*-Cre causes perinatal skeletal deformities that differ from abnormalities in post-natal mice

(A) Delayed osteoblast differentiation comparing Dicer$^{c/c}$ (1,3,5) and Dicer$^{\Delta oc/\Delta oc}$ (2, 4, 6). Alk Phos/Methyl Green staining in newborn caudal vertebrae (1, 2); E17.5 craniofacial regions (3, 4) and ribs (5, 6). (B) Reduced ex vivo differentiation of Dicer-ablated osteoblasts (right panel) revealed by Alk Phos (left panel). (C) Mechanism of defective Dicer$^{\Delta oc/\Delta oc}$ osteoblast maturation. Reduced osteoblast markers *Runx2, Osterix, Alk Phos* and *OC* after the proliferation period (day 7). Reduced let-7a expression and consequent upregulation of *Col1a1* confirm the loss of Dicer processing.

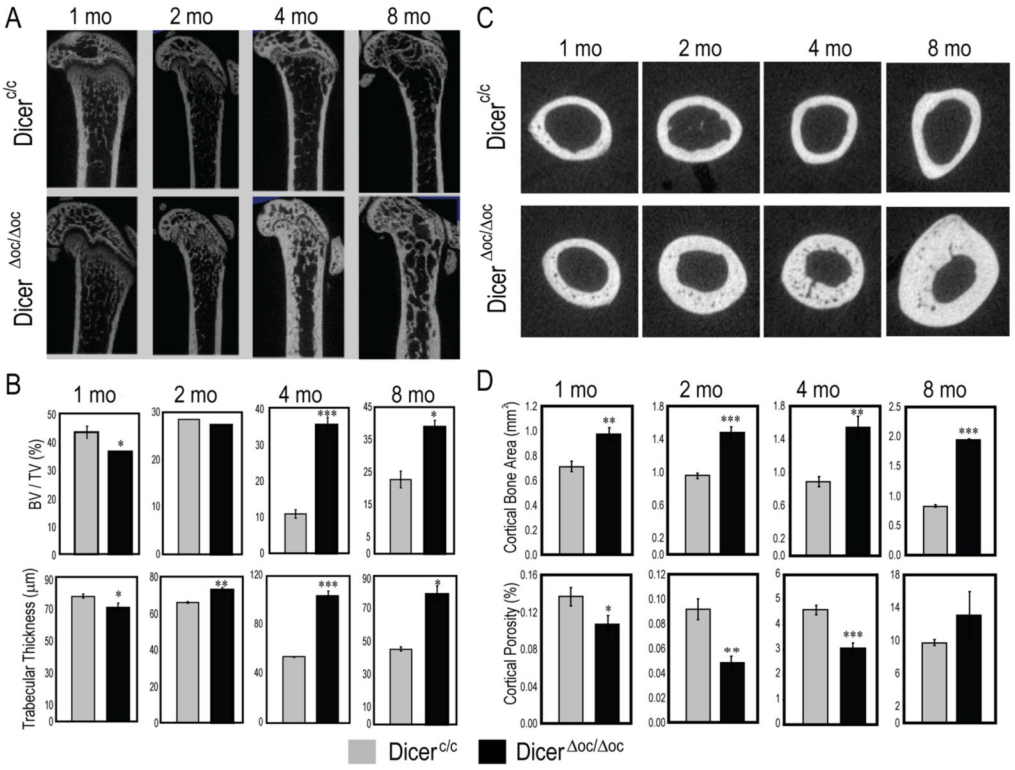

Figure 5. High bone mass phenotype in adult mouse caused by *Dicer* excision by *OC*-Cre

(A) Femur mid-bone sagittal μCT sections show mineralized trabecular and cortical bone at the indicated ages. (B) Quantitation of trabecular bone parameters. Reduced trabecular bone in femurs of 1 month $Dicer^{\Delta oc/\Delta oc}$ (%BV/TV) is significantly normalized by 2 months and significantly increased at 4 and 8 months compared to control $Dicer^{c/c}$ bone. (C) Transverse scan of femurs at mid-diaphysis. (D) Quantitation of cortical bone parameters shows significant increase in corical bone area (a volume parameter) with decreased porosity, especially at 2, 4 and 8 months in $Dicer^{\Delta oc/\Delta oc}$ mice. Values are mean±SD (n=3 mice), *** p-value <0.001, ** p-value <0.005, * p value <0.05.

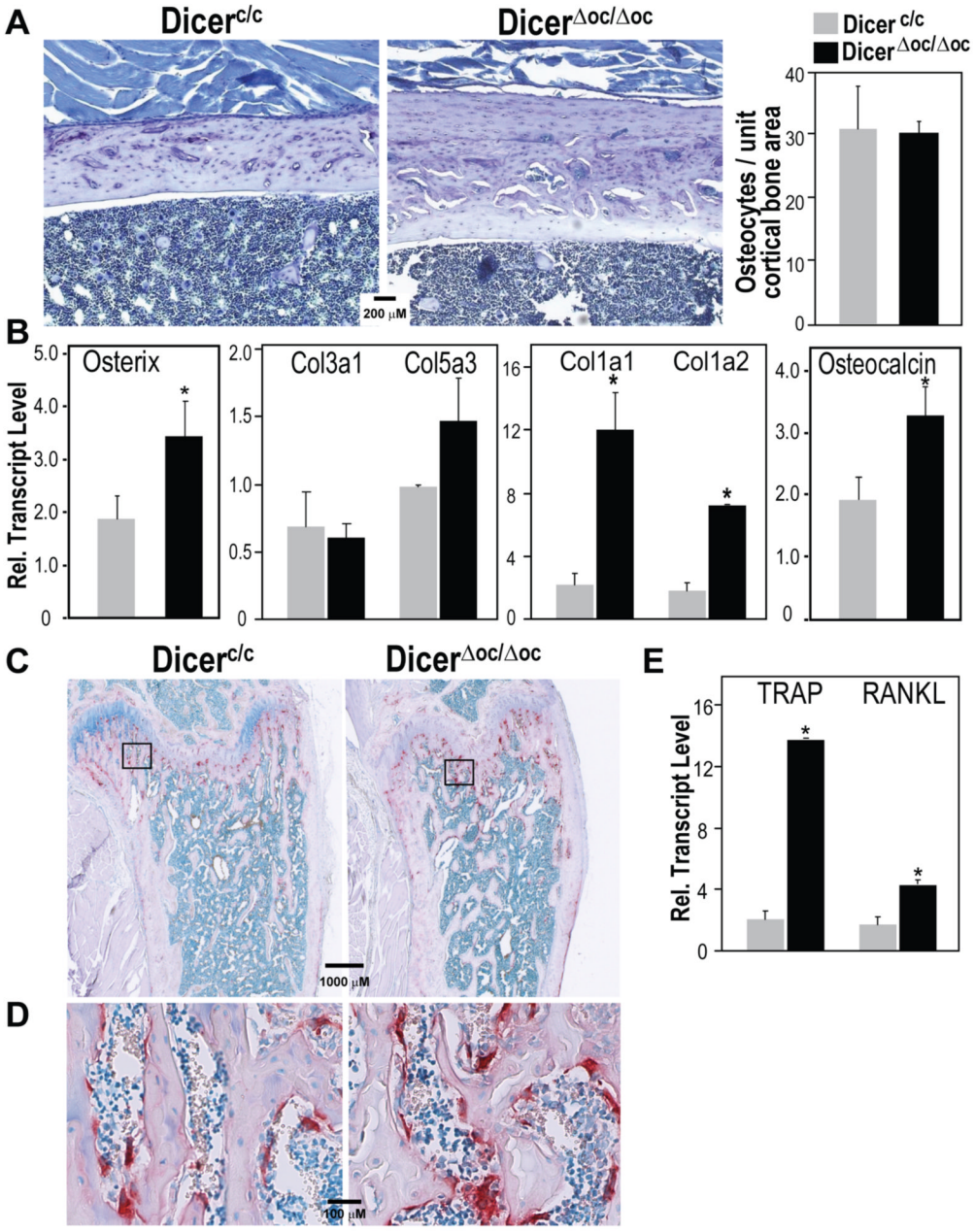

Figure 6. Normal bone content in Dicer$^{\Delta oc/\Delta oc}$ adult mice

(A) Left panels—Toluidine blue stained sections of mid-shaft cortical bone from control and Dicer$^{\Delta oc/\Delta oc}$ femurs at age 2 months. Right panel—Normal density of osteocytes as osteocyte counts (lower panel) at 2 month of age. (B) Total cellular RNA prepared from 4 month age tibia bone (n=4 mice per group) for gene expression of bone-specific collagen (Col1a1, Col1a2 and Col5a3) and the immature collagen (Col3a1). (C) Increased osteoclast activity coupled to increased bone formation shown by TRAP staining of whole femur at 2 month and (D) magnified trabeculae showing TRAP positive cells. (E) Expression of TRAP and RANKL mRNA by qRT-PCR. Values are mean±SD (n=3 mice), *** p-value <0.001, ** p-value <0.005, * p value <0.05.

Table 1

List of primers used for quantitative real time PCR.

Gene	Primer Sequence
Runx2	For 5′CGCCCCTCCCTGAACTCT 3′ Rev 5′ TGCCTGCCTGGGATCTGTA 3′
Alkaline phosphatase	For 5′ TTGTGCGAGAGAAAGGAGA 3′ Rev 5′ GTTTCAGGGCATTTTTCAAGGT 3′
Osteocalcin	For 5′ CTGACAAAGCCTTCATGTCCAA 3′ Rev 5′ GCGCCGGAGTCTGTTCACTA 3′
Collagen1a1	For 5′ CCCAAGGAAAAGAAGCACGTC 3′ Rev 5′ AGGTCAGCTGGATAGCGACATC 3′
Collagen1a2	For 5′ GTCCTAGTCGATGGCTGCTC 3′ Rev 5′ CAATGTCCAGAGGTGCAATG 3′
Collagen3a1	For 5′ AGGCCAGTGGCAATGTAAAG 3′ Rev 5′ CTCCATTCCCCAGTGTGTTT 3′
Collagn5a3	For 5′ AGGGACCAACTGGGAAGAGT 3′ Rev 5′ AAAGTCAGAGGCAGCCACAT 3′
Bone Sialoprotein	For 5′ GCACTCCAACTGCCCAAGA 3′ Rev 5′ TTTTGGAGCCCTGCTTTCTG 3′
Osteopontin	For 5′ ACTCCAATCGTCCCTACAGTCG 3′ Rev 5′ TGAGGTCCTCATCTGTGGCAT 3′
TRAP	ABI mm00475698_m1
RANKL	ABI mm00437135_m1
Dicer	For 5′ GGTGGTTCGTTTTGATTTGCC 3′ Rev 5′ GGCAGTGTTGATTGTGACTC 3′
P21	For 5′ TTGCACTCTGGTGTCTGAGC 3′ Rev 5′ TCTGCGCTTGGAGTGATAGA 3′